Advances in Natural Sciences:
Nanoscience and Nanotechnology

Effect of coating mild steel with CNTs on its mechanical properties and corrosion behaviour in acidic medium

To cite this article: Mahmud Abdulmalik Abdulrahaman *et al* 2017 *Adv. Nat. Sci: Nanosci. Nanotechnol.* **8** 015016

OPEN ACCESS
IOP Publishing
Advances in Natural Sciences: Nanoscience and Nanotechnology
Adv. Nat. Sci.: Nanosci. Nanotechnol. **8** (2017) 015016 (14pp)
https://doi.org/10.1088/2043-6254/aa5cf8

Effect of coating mild steel with CNTs on its mechanical properties and corrosion behaviour in acidic medium

Mahmud Abdulmalik Abdulrahaman[1], Oladiran Kamaldeeen Abubakre[1,4], Saka Ambali Abdulkareem[2,4], Jimoh Oladejo Tijani[3,4], Ahmed Aliyu[2] and Ayo Samuel Afolabi[5]

[1] Department of Mechanical Engineering, Federal University of Technology, PMB 65, Gidan Kwano, Minna, Niger State, Nigeria
[2] Department of Chemical Engineering, Federal University of Technology, PMB 65, Gidan Kwano, Minna, Niger State, Nigeria
[3] Department of Chemistry, Federal University of Technology, PMB 65, Bosso Minna, Niger State, Nigeria
[4] Nanotechnology Research Group, Centre for Genetic Engineering and Biotechnology (CGEB), Federal University of Technology, PMB 65, Bosso Minna, Niger State, Nigeria
[5] Department of Chemical, Materials and Metallurgical Engineering, Botswana International University of Science and Technology, Plot 10071, Boseja ward, Palapye, Botswana

E-mail: afolabia@biust.ac.bw

Received 6 September 2016
Accepted for publication 31 October 2016
Published 3 March 2017

Abstract

The study investigated the mechanical properties and corrosion behaviour of mild steel coated with carbon nanotubes at different coating conditions. Multi-walled carbon nanotubes (MWCNTs) were synthesized via the conventional chemical vapour deposition reaction using bimetallic Fe–Ni catalyst supported on kaolin, with acetylene gas as a carbon source. The HRSEM/HRTEM analysis of the purified carbon materials revealed significant reduction in the diameters of the purified MWCNT bundles from 50 nm to 2 nm and was attributed to the ultrasonication assisted dispersion with surfactant (gum arabic) employed in purification process. The network of the dispersed MWCNTs was coated onto the surfaces of mild steel samples, and as the coating temperature and holding time increased, the coating thickness reduced. The mechanical properties (tensile strength, yield strength, hardness value) of the coated steel samples increased with increase in coating temperature and holding time. Comparing the different coating conditions, coated mild steels at the temperature of 950 °C for 90 min holding time exhibited high hardness, yield strength and tensile strength values compared to others. The corrosion current and corrosion rate of the coated mild steel samples decreased with increase in holding time and coating temperature. The lowest corrosion rate was observed on sample coated at 950 °C for 90 min.

Keywords: carbon nanotubes, coating, corrosion, mechanical properties
Classification numbers: 1.00, 2.04, 2.05, 5.08, 5.09

1. Introduction

Mild steel remains an important engineering material frequently applied in construction, chemical, power production, automobile and electrochemical industries due to its abundance at relatively low production cost. Above all, mild steel possesses unique and remarkable mechanical properties such as good strength, toughness, ductility, formability and weldability which confirm its suitability as a better construction material in comparison to other engineering materials [1–3].

In fact, most fabricators and machinists consider mild steel as a favourite raw material in the production of engineering components such as gears, cams, shafts, keys, hand tools among others. Some of these engineering components must have strong and hard surface along with soft and tough core for their durability, reliability and safe operations depending on the operational conditions. These aforementioned properties are however lacking in mild steel, thus causing simultaneous wear at the surface and subsequently breakage upon impact during operations [4, 5]. Furthermore, mild steels are sometimes susceptible to ravages and failure depending on the environmental conditions causing deterioration of material surfaces, a phenomenon called corrosion. Corrosion causes gradual weakening and failure of material properties which can sometimes lead to human injury, loss of life and collateral damage [6]. In fact, William and David [2] and Singh *et al* [7] independently found that about 5% income of the developed nations were spent on corrosion prevention and maintenance and/or replacement of products lost due to the effect of corrosion. It should however be mentioned that, corrosion of steels in acidic aqueous solution is evident in most industries where acids are used in pickling, industrial cleaning, descaling and oil well acidizing processes [8].

On the other hand, several metals and non-metals, ceramics including polymers have been applied as coating on mild steel to improve their hardness, wear, fatigue and corrosion resistance in order to suit many applications [9, 10]. Montemor [9] reported that utilizing conductive fillers such as carbon black, graphite, fullerene, metallic particles and carbon nanotubes should improve the surface properties of materials.

Of all these coating materials or conductive fillers, carbon nanotubes (CNTs) are considered the most promising nanomaterials to improve the surface properties of existing materials due to its exceptional electrical, mechanical, chemical and thermal properties [10, 11]. Several synthesis approaches such as electrical arc discharge, laser ablation, pyrolysis, plasma enhanced, thermal or catalytic chemical vapour deposition have been explored to produce high quality CNTs of different length and diameter. However, catalytic chemical vapour deposition (CCVD) is considered more versatile and prominent than other methods for obtaining large-scale and high quality CNTs at comparatively low cost [12]. A typical CCVD technique involves decomposition of carbon sources (acetylene or methane gas) at a temperature above 600 °C on metals such as Fe, Co, Mo, Ni or their mixtures placed on a quartz boat in a horizontal quartz tube inside furnace at a predetermined time. Sometimes, these metallic particles are supported on conventional substrates such as $CaCO_3$, SiO_2, MgO, Al_2O_3, TiO_2, zeolites, activated carbon, and clay to produce the CNTs. Conversely, purification of CNTs grown on substrates remains a challenge after production, which often involves several steps. Different purification methods have been utilised still concentrated HNO_3 or mixture HNO_3–H_2SO_4 remains most frequently used. Although, this purification method has certain drawbacks limiting the purified CNTs from fulfilling all require technical processing.

Furthermore, the choice of CNTs as a coating material includes ultra-strength and ability to tolerate large strain as reinforcing materials in polymer composites [13]. Chen *et al* [14] revealed that the surfaces of metals possess defects, cracks, gaps, crevices and micro holes, which behave as active sites for initiation of fatigue and dissolution of metal during corrosion. Thus, CNTs can easily be made to enter and fill in these micro holes acting as a physical barrier to propagation of cracks and corrosion processes. Poole and Owens [15] found that the tensile strength of steel incorporated with 30% CNTs was seven times higher than the original steel without CNTs. The service conditions of many engineering materials make it necessary for them to possess a very strong and solid surface to resist wear, leaving a softer and more plastic core to absorb shock upon impact during operations [16, 17].

Furthermore, many surface treatment methods have been developed and applied to enhance the surface properties of components produced from mild steel. For instance, the surface properties of mild steel can be improved via the diffusion of carbon, nitrogen, carbon nitride or cyanide onto the surface of mild steel at austenitising temperature and/or lower temperature. Although, Qi *et al* [17] highlighted several limitations of diffusion methods to include: time and energy consumption, complex heat treatment schedules, wider heat affected zone, lack of solid solubility limited and slower kinetics. Besides, the method is not environmentally friendly. In addition, metals such as zinc, chromium, titanium and their alloys have been deposited as coating on mild steel to improve its surface properties. Marder [18] found zinc to be less ductile compared to the substrate it protects thus compromising the coating intension during deformation. Chromium because of its desired properties has been used to coat mild steel but this method was restricted due to health and environmental concerns [19]. Deposition of ceramics and their composites as coating on mild steel have been reported to enhance the surface properties of mild steel. However, ceramic coatings have certain limitations such as high cost of equipment, low coating adherence, large porosity, requirement of controlled environment (such as vacuum) and line of site. Moreover, complex procedures are often involved during operations [20].

In view of the associated deficiencies and challenges with the existing coating methods to improve the performance of mild steel, it is imperative to develop simple, scalable, cheap and environmental friendly method for the surface treatment of mild steel that will impact superior surface properties. Therefore, this study investigated the influence of CNTs at different coating conditions on the mechanical properties and corrosion behaviour of mild steel in acidic medium.

2. Materials and methods

2.1. Materials and sample preparation

All the chemicals used in this study are of analytical grade with percentage purity in the range of 96–99%. They included $Fe(NO_3)_3.9H_2O$, $Ni(NO_3)_3.6H_2O$, acetone, ethanol, sodium hydroxide (NaOH), hydrochloric acid (HCl), sulphuric acid (H_2SO_4) and nitric acid (HNO_3). Acetylene and argon gases were obtained from BOC Nigeria and they were of analytical grade with percentage purity of 99%. Emery papers of 220, 320, 400, 600, and 800 grits, polyester resin, methyl ethyl ketone, cobalt naphthalene, copper wire, PVC pipe and gum arabic (GA) were also used in the experimentation.

The as-received mild steel sample of 16 mm diameter was purchased from Kakuri industry stock market in Kaduna state, Nigeria and was cut and machined to American Society for Testing and Materials (ASTM) standard for the mechanical properties (tensile strength, impact energy and hardness) and corrosion behaviour tests that were to be carried out. According to ASTM standard sample dimensions, the length of mild steel required for this work was calculated to be 2 m including allowances for cutting and supporting tools during cutting and machining. In order to relieve the samples from induced stress due to machining, the samples were normalised by heating them in muffle furnace to austenitic temperature of 950 °C and held for 30 min and thereafter cooled in still air.

The samples were wire brushed and polished with series of emery paper (240, 320, 400, 600 and 800 grits) until a fairly smooth and mirror like surface was obtained. The samples were then cleaned with acetone to remove grits particles and grease that might have stocked and/or stained the samples during polishing.

2.2. Synthesis of carbon nanotubes

This study employed the catalytic vapour deposition method for the synthesis of carbon nanotubes. Carbon nanotubes were synthesized by the decomposition of acetylene (C_2H_2) in a tubular quartz reactor placed horizontally in a furnace. The furnace was electronically controlled such that the heating rate, reaction temperature and gas flow rates could be accurately maintained as desired. The catalyst (Fe–Ni/kaolin) was loaded into a quartz boat ($120 \times 15\,mm^2$) at room temperature and the boat was placed in the centre of the quartz tube. The furnace was then heated at 10 °C min^{-1} while argon was flowing over the catalyst at 300 ml min^{-1}. Once a temperature of 750 °C was attained, the argon flow rate was reduced to 230 ml min^{-1} and C_2H_2 was then introduced at flow rate 200 ml min^{-1} for a period of 60 min. The C_2H_2 flow was stopped after this reaction period and the furnace was allowed to cool to room temperature under a continuous flow of argon. The boat was then removed from the reactor. The CNTs synthesized were then characterized to determine their morphology, crystallinity and thermal stability by means of high resolution scanning electron microscopy (HRSEM) and energy dispersive x-ray analysis (EDX) using equipments of Zeiss Auriga, x-ray diffraction (XRD) using PW1800 diffractometer, differential thermogravimetry (DTG) and thermogravimetric analysis (TGA) using Perkin Elmer TGA 4000, respectively. The synthesized CNTs were first boiled in a 30% aqueous HNO_3 solution for 9 h to remove C-based impurities. Thereafter, washed in deionised water and dried at 100 °C, the treated sample was heated at 30 °C for 45 min in a flowing argon atmosphere (500 ml min^{-1}) to remove active oxygenated groups, induced during HNO_3 treatment [21]. The resultant oxidized CNTs were purified with 30% aqueous HNO_3 at 100 °C, stirred for 2 h and washed with distilled water to obtain neutral pH value. The raw and purified CNT samples were characterized using HRSEM and HRTEM.

2.3. Dispersion of carbon nanotubes

The dispersion of purified CNTs was achieved using ultrasonicator bath and gum arabic (GA). A known weight (10 g) of GA was dissolved in 100 ml of distilled water in a 500 ml beaker and subsequently stirred for 30 min using magnetic stirrer. Thereafter, samples of CNTs were then added to the mixture and stirred for 60 min. The concentration of CNTs was kept at 0.25 g on 1 g of GA. The stirred mixture was characterized using zetasizer to establish a basis for comparison with the mixture after sonication. The stirred mixture was then placed in ultrasonicator bath and the water in the bath was adjusted to be at the same level with mixture in the beaker. The bath was set to sonicate for 90 min, and thereafter the dispersed CNTs was again analysed with zetarsizer. The slurry was further ultrasonicated for 6 h after which it was centrifuged at 3000 rpm for 15 min to remove the undispersed CNTs. The stability of the dispersed CNTs in water, ethanol and GA was also observed for a period of one month. The resulting dispersed CNT slurry was characterized using Fourier transform infrared (FTIR) spectroscopy to identify the functional groups induced on the CNTs by the surfactant.

2.4. Coating of mild steel samples with purified CNTs

The prepared steel samples were dipped into the CNTs slurry, removed and dried at 80 °C for 15 min in furnace to remove the water in the coating. The coating and drying were repeated three times to increase the CNTs loading on the samples. The samples were grouped into six with at least three samples for each experiment that were to be carried out. The coated samples were then heated to austenitic temperature (900 °C) in vacuum furnace and homogenized for 30 min. The samples were allowed to cool in the furnace and were removed to test their mechanical properties, corrosion behaviour and morphology analysis. The treatment was repeated with different sets of samples for soaking times of 60 and 90 min and also at different austenitic temperature of 950 °C and holding times of 30, 60 and 120 min.

2.5. Determination of mechanical properties of the coated steel samples

The tensile strength of the coated (and control) samples was determined using Hounsfield tensometer. The tensile test sample was inserted in the testing machine using split chucks and pins.

Table 1. Percentage elemental composition of mild steel sample.

Element	Fe	C	Si	Al	Cr	Ca	Mn	Mo	Others
Weight (%)	96.29	0.07	0.13	0.2	0.04	0.15	0.46	0.21	2.45

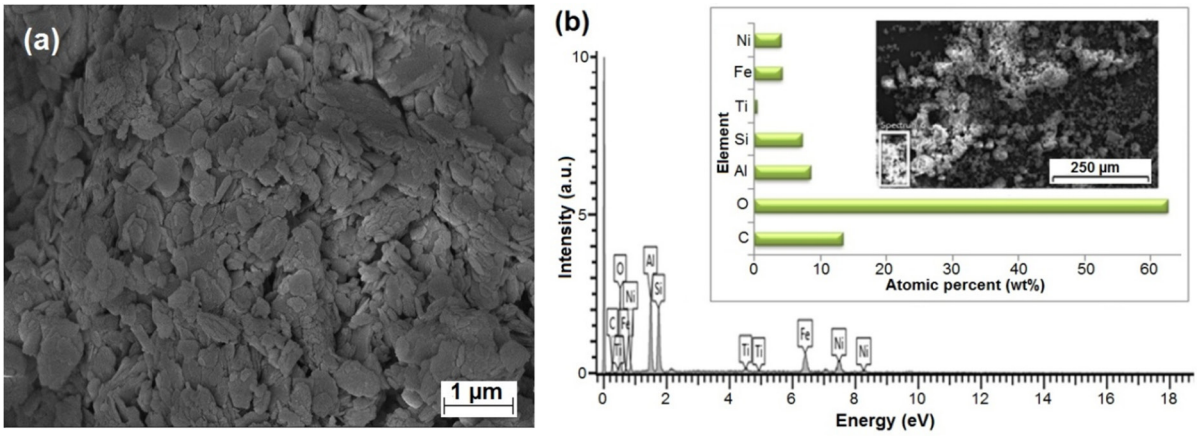

Figure 1. (a) HRSEM and (b) EDX analysis of the prepared Fe-Ni catalyst supported on kaolin.

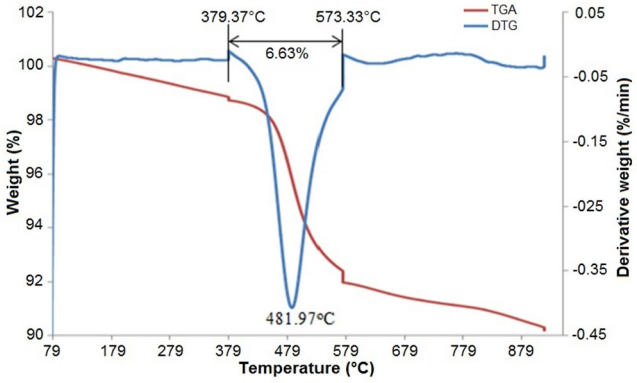

Figure 2. TGA and DTG analyses of Fe-Ni/kaolin catalyst after calcinations.

The drives system on the machine was adjusted to ensure proper grip of the sample and to take off slack. The mercury column was set to zero before the load was applied. The autographic record drum that was wrapped with graph sheet was set such that a perpex indicator was at zero and the picker also at zero axis of the graph sheet. The load-extension plot was traced by sliding the mercury indicator and depressing the picker on the graph sheet wrapped on the rotating drum while the load was gradually and continuously applied through the loading handle until failure of the sample occurred. The load-extension data on the resulting graph sheet and the sample parameters were used to evaluate the ultimate tensile strength, modulus of elasticity, percentage elongation and percentage reduction in area.

The Vickers micro hardness test was used to determine the surface micro hardness values of the steel samples. The surfaces of the treated samples were subjected to a compressive load of 1.96 N for 15 s loading time using Shimadzu HMV-2000 micro hardness tester. A diamond shape indenter with square-based pyramid with an angle of 136° between opposite faces was used. At least three measurements were taken on each sample and the average was used to evaluate the micro hardness of the treated materials. For the basis of comparison, the micro hardness of the control sample was also measured. The Vickers hardness ($HV_{0.2}$) was calculated using equation

$$HV_{0.2} = \frac{F}{A} \approx \frac{1.8544F}{d^2}, \quad (1)$$

where F is the applied load in N, A is the surface area of the resulting indentation in mm^2 and d is the length of the diagonal of the resulting indentation in mm [22]. The impact energy of the treated mild steel samples was evaluated using Hounsfield balance impact test machine. The machine was designed to have two opposite swinging hammers that can pass each other during operation; one of the hammers contains the sample holder and a wedge to keep the sample in position. During the test, the hammers were raised to the required height and held in position by a link mechanism at the top of the machine. The sample which was machined to ASMT standard ($8 \times 45\,mm^2$, with a notch depth of 2 mm and notch tip radius of 0.02 mm at an angle of 45°) was placed and gripped in the sample holder; the hammers were then released to strike the sample as they pass each other. The energy in foot pound that was absorbed in breaking or bending the sample was recorded and the impact strength in Joules meter was evaluated.

2.6. Electrochemical corrosion test on coated steel samples

The electrochemical behaviour of the CNT-coated steel samples was studied at room temperature (25 °C) in 0.5 M H_2SO_4 using a 3-electrode cell polarization method consisting of platinum grid as counter electrode, a saturated calomel electrode (SCE) as reference electrode and the coated mild steel samples as the working electrode. The measurements were carried out using a potentiostat/galvanostat EGG 273A coupled to a frequency response analyzer (FRA) EGG 1025. The potential (E) of the working electrode was scanned from −2.5 to +0.5 V at steps of 5 mV s^{-1}.

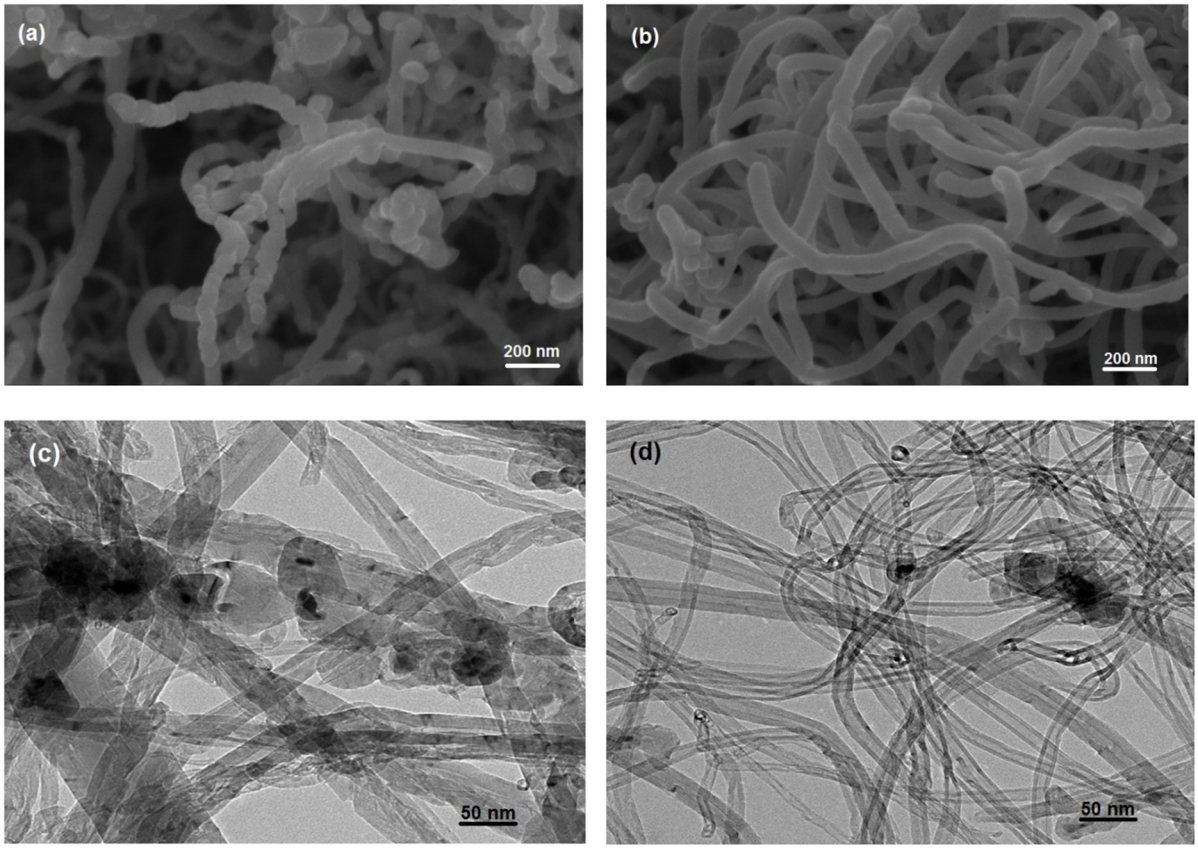

Figure 3. HRSEM results of (a) as-produced CNTs soot, (b) purified CNTs; (c) HRTEM micrograph of as-synthesized CNTs and (d) purified CNTs.

3. Results and discussion

3.1. Synthesis and purification of carbon nanotubes

The elemental composition of the raw sample was determined using x-ray energy fluorescence spectrometer and the results obtained are presented in table 1. It has been reported that steel with carbon content ⩽0.25% is categorised as low carbon steel otherwise called mild steel. It can be inferred from the results in table 1 that the sample utilised in this study is mild steel since the carbon content of the sample is 0.07%. Besides carbon, there is presence of other elements such as Si, Al, Cr, Ca, Mn and Mo in different proportions.

In this study a bimetallic (Fe-Ni) catalyst was wet impregnated on the surface of kaolin to prepare the catalyst used in the synthesis of CNTs. The choice of Fe-Ni as the catalyst was favoured by their high solubility and high rate of diffusion of carbon through them at high temperature [23]. Figures 1(a) and (b) display the HRSEM micrograph and EDX data of the prepared catalyst used to grow the CNTs.

The HRSEM micrograph of the prepared catalyst showed the presence of agglomerated flake-like morphology with the metal catalyst particles homogeneously distributed on the surface of the kaolin support. As expected, the EDX result reveals the presence of Fe and Ni which can be traced to the Fe and Ni precursor compounds used in the preparation of the catalyst. Other elements detected include aluminium, silicon, titanium and oxygen that can be traced to the kaolinite ($Al_2Si_2O_5(H_2O)_4$) which form the principal mineral in kaolin. The carbon detected was either from holey carbon grid or possibly from kaolin. The percentage elemental compositions of the prepared catalyst were also evaluated and the result shows that the catalyst contains 16.14% C, 8% Al, 6.93% Si, 2.6% Fe, 2.34% Ni, 63.69% O and 0.31% Ti. On the specific surface area of the catalyst using Brunauer-Emmett-Teller (BET), results obtained indicate that the specific surface area of the prepared bimetallic catalyst was 3.76 $m^2\ g^{-1}$ which is however low when compared to the 12.55 $m^2\ g^{-1}$ obtained for kaolin (support). This is an indication that the metal particles were distributed inside the pores of the kaolin rather than the external surface which suggest the rigidity of the prepared catalyst and cannot be easily washed off during the production of carbon nanotubes. Furthermore, the thermal profile of the prepared catalyst at different temperature was investigated. Figure 2 represents the TGA and DTG results of the prepared catalyst after calcined at 500 °C for a period 16 h. According to figure 3, it can be seen that there was no observable weight loss from 30 to 100 °C, which possibly suggests absence of water molecules and nitrate from the sample. The weight loss of approximately 6.63% occurred at a temperature range of 379.37–573.33 °C and can be ascribed to the decomposition of the prepared catalyst leading to the deposition of $NiFe_2O_4$ component on the kaolin support. This compound ($NiFe_2O_4$) ceased around 573.33 °C and confirmed the stability of $NiFe_2O_4$ at higher temperature without any oxygen vacancy formation.

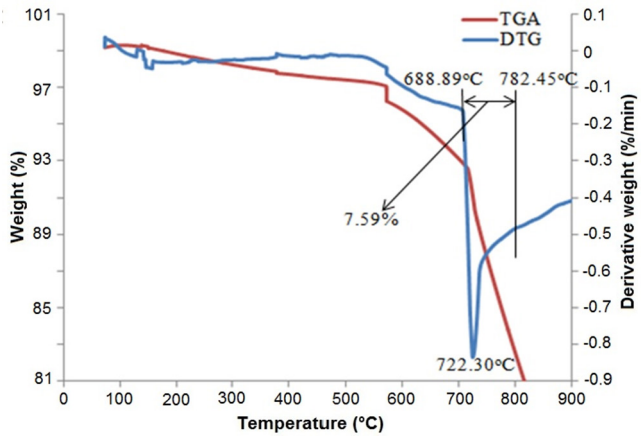

Figure 4. TGA profile of purified CNT samples.

The catalyst prepared was further utilised to produce CNTs via catalytic vapour deposition method and the characterization results are presented. Figures 3(a) and (b) show the HRSEM images of the as-synthesized and purified CNTs respectively. The image in figure 3(a) resembles randomly distributed tube–like structures having few agglomerated branches and tiny particles on the surface. These branches and particles are regarded as defects and impurities which can affect the desired mechanical and electrical properties of the CNTs. Saifuddin *et al* [24] reported that the impurities commonly observed in synthesized CNTs are mostly amorphous carbon, unwrapped graphite, metal catalyst, small fullerenes and some dangling bonds. The metal catalyst in this case cannot be seen in the SEM analysis as they are covered by the walls of the tubes. On the other hand, in figure 3(b) a clear defined long tubular morphology with less agglomeration and less presence of catalyst metallic particles can be observed, which confirms the effectiveness of the adopted purification process.

The CNTs produced were further analysed with high resolution transmission electron microscopy (HRTEM) to determine the nature of the product. The HRTEM images presented in figures 3(c) and (d) show that the CNTs produced are multiwalled carbon nanotubes with hollow structure, inner diameter and length of several nanometres. The micrographs presented in figure 3(c) represents the as-synthesized CNTs on the surface of Fe-Ni/kaolin catalyst, which contain impurities such as the metals catalyst on the surface of CNTs. Figure 3(d) reveals the HRTEM image of the purified CNTs after two steps oxidation. It can be observed from the figure 3(d), that the image of the purified carbon material reveals clean-surfaced CNTs which can be attributed to the oxidation of impurities such as amorphous carbon, unwrapped graphite sheet and small fullerenes which form the main constituents of the impurities aside the metal catalyst. The high concentration acid has expected, dissolved and removed most the metallic impurities to the minimum possible level except the little ones encapsulated on the matrices of the tubes during CNTs growth. It is also apparent that figure 3(d) contains long parallel graphitized sheets forming CNT walls and tubes with several opening pores than figure 3(c) due to the purification process. The HRTEM analysis further complements the HRSEM result on the purified CNTs shown in figure 3(b).

Furthermore, the thermal stability and specific surface area of the purified CNTs produced were investigated using TGA and nitrogen adsorption BET. The TGA analysis (figure 4) indicates two degradation temperatures firstly at 230.83–269.91 °C with a corresponding weight loss of 0.188%, which can be attributed to the loss of carbonaceous materials. Thereafter, no significant weight loss was observed before 622.91 °C, which indicates that the purified CNTs are free of amorphous carbon. However, at the degradation temperature range of 622.91–861.67 °C, 12.46% weight loss was observed as shown in figure 4, which is typical decomposition profile for multiwall carbon nanotubes [25]. This analysis further reveals that the synthesized CNTs are suitable for metal coating. It can also be seen from figure 4 that after the purification process, the thermal stability and decomposition temperature of the CNTs increased from 672.79 to 722.30 °C and less than 8% weight loss was observed between 688.89–782.45 °C. The TGA results demonstrate that most metallic nanoparticles and residual support materials which served as impurities were clearly removed to a reasonable level.

The specific surface areas of the purified CNTs were also determined for the purpose of investigating the influence of purification on the surface properties of the CNTs. The BET surface area of the raw CNTs was found to be 244.4 $m^2\ g^{-1}$, while that of the purified CNTs was 268.40 $m^2\ g^{-1}$. The higher BET surface area of the latter than the former was due to the removal of the impurities such as the residual catalyst and amorphous carbon in the as-synthesised CNTs.

3.2. Dispersion study of CNTs in solvents and surfactant

In order to select the best dispersant for CNTs in this study, the as-synthesised purified CNTs were dispersed in different solvents such as water, ethanol and water/gum arabic solution and subjected to ultrasonication for 2 h. The results obtained in the order dispersion (CNTs/water, CNTs/ethanol and CNTs/gum arabic) are presented in figure 5(a). Previously, Peng *et al* [25] had proved that CNTs can be readily dispersed in water, ethanol and water/GA mixture. Similarly, Xin *et al* [25] concluded that dispersion of CNTs in some solvents especially water produced a kinetically stable system than a thermodynamically system, nevertheless aggregation and sedimentation later occurred with time. Figure 5(b) shows the state of dispersion after ageing for 2 h. It can be seen from this figure that CNTs dispersed in water showed high level of re-agglomeration and sedimentation coupled with poor wettability of CNTs in water. It is evident from the results presented that certain quantities of CNTs were suspended on the surface of the water while others settled at the bottom of the vial. In addition, a clear portion was obtained in between the CNTs floated at the top and CNTs settled at the bottom. However in ethanol solvent, the CNTs were uniformly dispersed and remained so even after 2 h. A closed observation of the vial belonging to CNTs/ethanol mixture revealed that the dark colour in the liquid started fainting from the top to the bottom of the vial, thus indicating sedimentation. The dispersion of CNTs in the mixture of water/gum arabic (water/GA) showed no difference compared to that observed in figure 5(a)

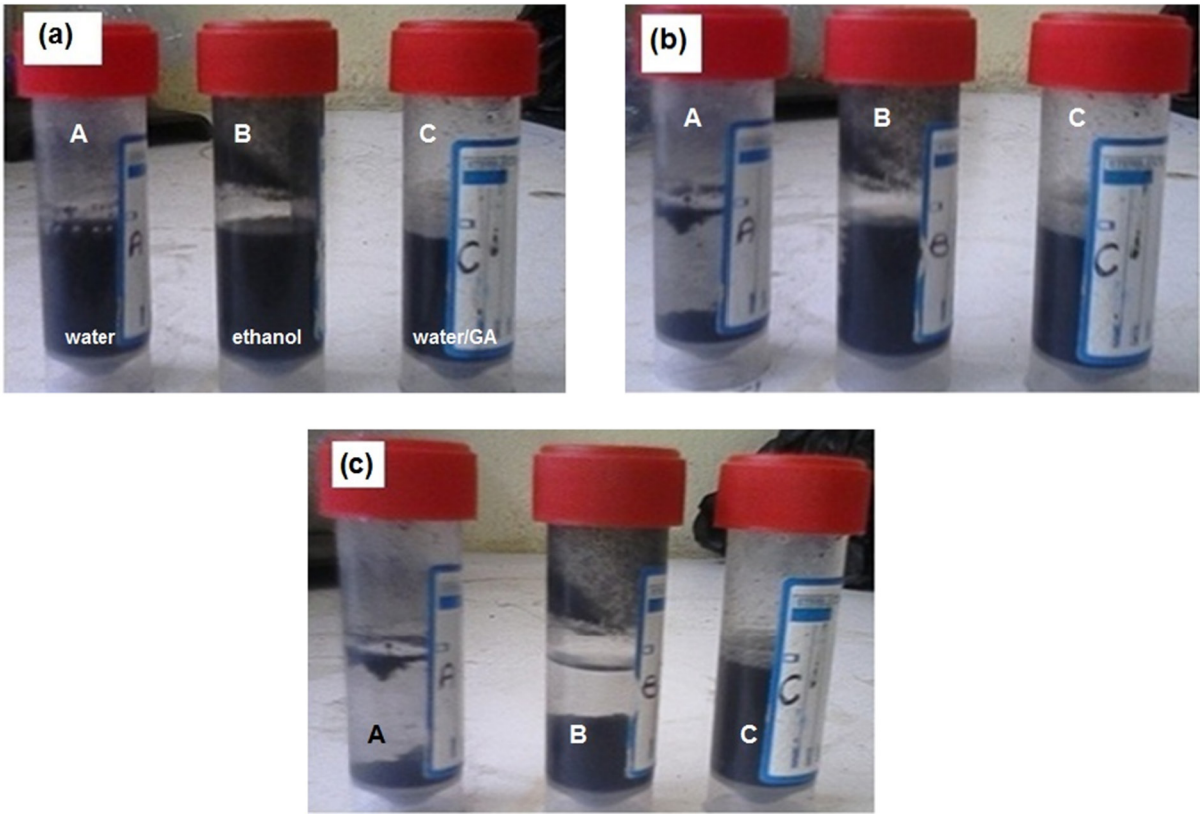

Figure 5. CNTs dispersion (a) immediately after sonication, (b) stability after standing for 2 h, and (c) stability after standing for 8 h.

for water (labelled A) and water/GA system (labelled C) dispersed in CNTs

Figure 5(c) shows the CNTs in the media after standing for 8 h. It can be seen that, the CNTs in vial A and B have settled due to combined action of gravity and van der Waals attraction forces on the surfaces of the CNTs. Although closer inspection of these vials showed that the CNTs in ethanol did not completely settle to the bottom of the vial but formed some cloud of suspended network of CNTs linked together. Additionally, the CNTs in vial A was also not entirely settled, as some fractions of CNTs were either settled at the top or bottom. The CNTs in vial C remained uniformly dispersed even after a month, with little sedimentation observed at the bottom when the mixture was transferred to another container. The stability of CNTs in the mixture of water/GA can be explained in terms of the physical adsorption of the GA to the surface of the CNTs. In the process of the ultrasonication, the induced energy separated CNTs from their bundles and the GA was adsorbed and coated on the surfaces of the CNTs. The GA coating lowered the surface tension of the CNTs thereby preventing the formation of aggregates. The van der Waals attraction on the CNTs' surfaces was neutralized by the electrostatic repulsion forces from the GA which favoured the choice of water/GA dispersant in this study. More so, the excellent properties of CNTs lies in its ability to exist in individual nanotubes, not in bundles or skeins, nevertheless their high aspect ratio and some of its physical properties promote high free surface energy. CNTs tend to reduce their surface energy by attracting one another thereby forming bundles and rope which are held together by van der Waals forces [27]. Another challenge encountered when working with CNTs, is linked to their atomically smooth surface which affect compatibility (due to absence of reactive group that can bond) with other materials [28]. Thus, in order to derive full benefit from CNTs, the agglomerated CNTs have to be broken off into individual tubes to achieve good dispersion and also their surfaces be treated to ensure proper bonding between the CNTs and the materials. However, many approaches have been developed to achieve good dispersion and proper bonding between the tubes and other materials. In this work, the dispersion of CNTs was achieved using ultrasonicator bath and gum arabic (GA) at different sonication times. The significance importance of aspect ratio, the dynamic light scattering (DLS) analysis of the CNTs/gum arabic/water slurry was used to study the level of separation of the CNTs off their bundles in the medium. The results show that the duration of ultrasonication significantly influenced the degree of dispersion of CNTs in the media, which was evident in the size distribution presented in figure 6. In dynamic light scattering (DLS) analysis of CNTs dispersion in GA/water slurry at different times, the average friction coefficient of CNTs (D_h) is calculated as follows

$$D_h = \frac{L}{\ln(L/d) + 0.32}, \tag{2}$$

where L is the length of CNTs obtained from the curve, d is the average diameter of the CNTs obtained from TEM micrographs, L/d is known as the aspect ratio.

The slurry mixture samples labelled A, DGA, and ARAB was sonicated for 360, 90 and 30 min respectively. All samples were centrifuged for 15 min at 1500 rpm. An evaluation of the

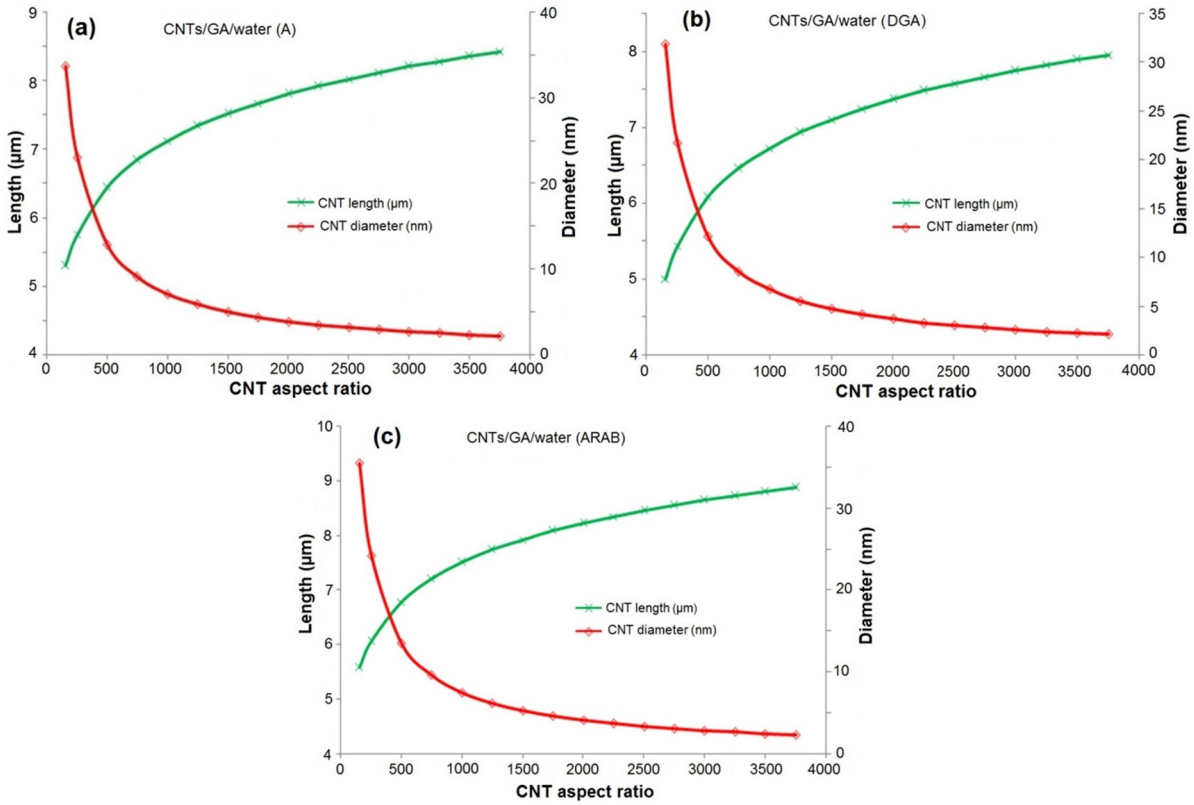

Figure 6. Dynamic light scattering (DLS) analysis of CNTs dispersion in GA/water slurry of samples labelled A, DGA and ARAB at different sonicated times: (a) 360 min, (b) 90 min, (c) 30 min with respectively of maximal length 8.43 μm, 7.96 μm, 8.80 μm and Z-average 986.2 nm, 931.3 nm, 1039 nm.

Table 2. Variation of elongation (%), reduction in area (%), yield strength and ultimate tensile strength with holding time at 900 °C and 950 °C.

Temperature (°C)	Holding time (min)	Elongation (%)	Reduction in area (%)	Yield strength (MN m^{-2})	Ultimate tensile strength (MN m^{-2})
Control		27.0	72.0	238.833	377.104
900	30	25.4	69.0	289.256	407.588
900	60	24.6	67.0	315.552	427.310
900	90	24.0	66.0	357.933	454.300
950	30	23.3	66.7	326.824	452.525
950	60	20.0	64.8	394.440	512.772
950	90	19.0	62.4	550.666	605.733

effects of sonication time on the dispersion of CNTs in the media showed that sonication time for proper dispersion of the CNTs in the slurry mixture exists between the minimum time (30 min) and the maximum time (360 min) considered. Although, the 30 min ultrasonication time was not sufficient to achieve individual separation of CNTs in the water/GA mixture due to strong hydrophobic nature of CNTs, physical sonication tends to cut CNTs or reduce their length sizes. In the same vein, short time was inadequate for dispersing the nanotubes in the slurry as revealed in the CNTs length of 8.8 μm, the longer time of 360 min probably provided much more favourable binding forces for molecular interaction or even improved functionalization beyond physical dispersion leading to longer lengths of CNTs. Functionalization is the addition of molecular functionalities of the media to the tip or sides of the CNTs. The best dispersion was achieved at 90 min and was considered as the optimum ultrasonication duration based on the moderate aspect ratio as shown in table 2. The length of CNTs in the slurry was about 7.96 μm. The possible explanation for this can be in terms of the explosive forces resulting from the collapse of bubbles formed during sonication process, thus causing shear separation of the outer CNTs from their bundles.

The slurry of the mixture of CNTs/water/GA was then used to coat the mild steel and calcined in the furnace at 900 °C for holding time of 30, 60 and 90 min. The HRSEM micrograph of the uncoated and CNTs coated mild steel samples calcined at 900°C for three different holding times is shown in figure 7. The HRSEM image (figure 7(a)) which represents an uncoated mild steel sample has smooth surface while deposit of white structures network of CNTs were noticed on the surface of coated mild steel samples (figures 7(b)–(d)).

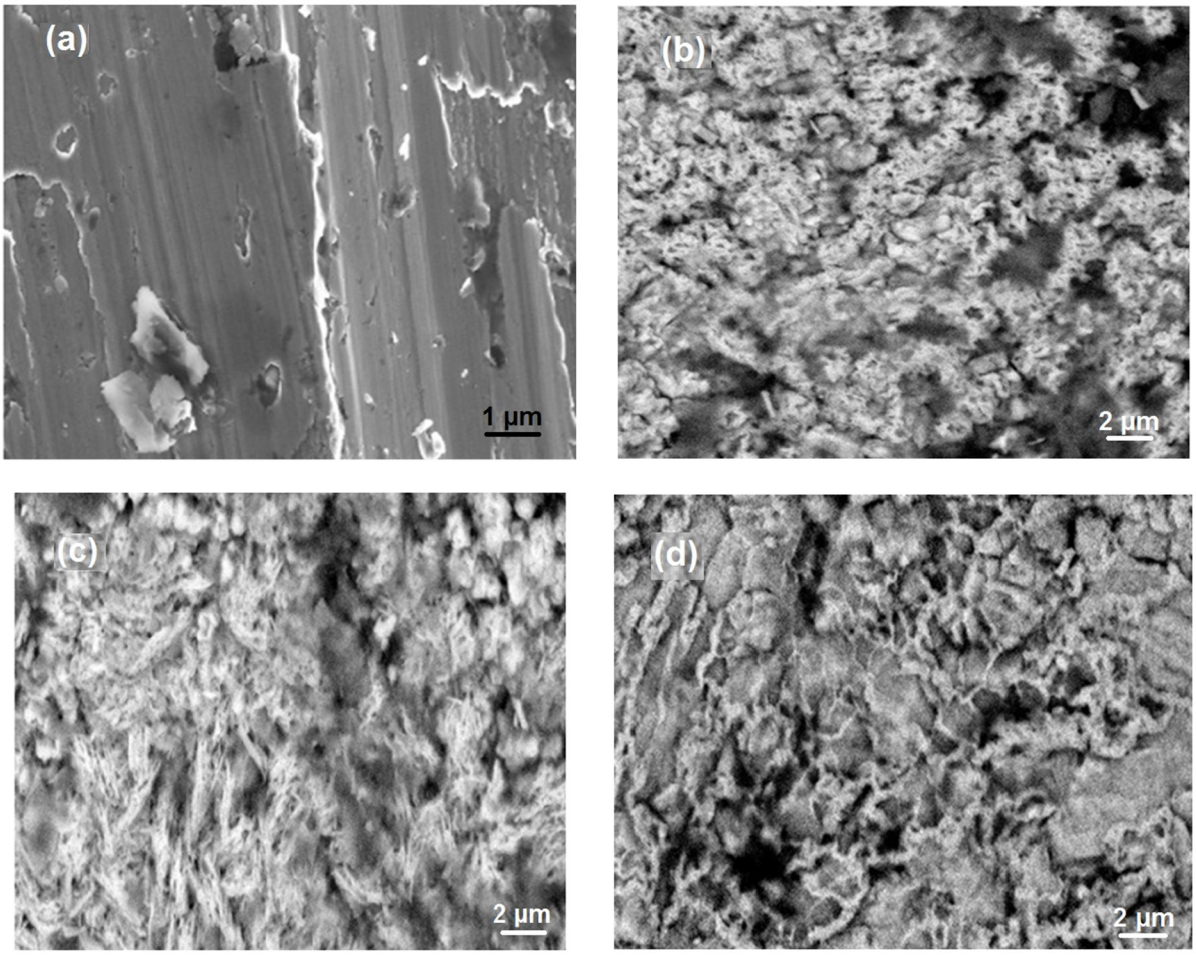

Figure 7. HRSEM micrograph of (a) uncoated mild steel sample, and coated mild steel sample treated at 900 °C for (b) 30 min, (c) 60 min and (d) 90 min.

A close observation of the HRSEM micrograph reveals that complete surface coverage of the mild steel with CNTs was not achieved, some dark spots not covered with CNTs were observed in figures 7(b) and (d) more than figure 7(c). These spots can be considered as points where excess GA in the CNTs slurry were concentrated and were burnt or perhaps removed due to the heating temperature in the furnace [29]. It was noticed that the density of the MWCNTs on the samples decreased with increase in holding time resulting in the decrease in coating thickness. The fibre and porosity analysis reveals that the predominant length of the CNTs fibre on the surface of the coated sample was in the range of 200 nm–1.5 μm. The pore sizes on the coated surface were found to be within the range 0.005 to 0.01 μm^2.

Figure 8 represents the HRSEM micrograph of the coated samples treated at calcination temperature of 950 °C for different holding times of 30, 60 and 90 min. For the mild steel samples calcined at 900 °C, the HRSEM micrograph reveals deposit of MWCNTs on the surface of the mild steel samples and also shows decrease in the density of the CNTs as the soaking time increased. Unlike what was obtained at 900 °C soaking temperature, different morphologies were noticed in the HRSEM images presented in figure 7. For instance, figure 8(a) which depicts holding time of 30 min indicates that during heating, part of the coated CNT on the surface of mild steel liquefied and later solidified after cooling to form considerable amount of woven-like pool structure and some tiny spherical particles. As the holding time increased to 60 min, more of the pool was formed which enveloped the coating material upon cooling (figure 8(b)). At 90 min holding time, complete evaporation of CNT/GA/water mixture from the mild steel was observed. The HRSEM micrograph is similar to that of uncoated mild steel; however residual tiny spherical CNTs or GA particles as indicated with an arrow on the surface of the sample.

3.3. Mechanical properties of the coated mild steel

The formed CNTs/GA/water slurry was used to develop film on mild steel samples and the coated samples were subjected to the following mechanical properties tests such as tensile, impact and hardness in order investigate the effect of the film on the properties of the mild steel sample.

Figure 9 depicts the sample coated with CNT/GA/water and thereafter annealed at 900 °C and 950 °C. Subsequently, the ultimate tensile strength of the samples annealed at 900 °C and 950 °C in the furnace for different holding times (30, 60 and 90 min) with respect to uncoated sample (control) are shown.

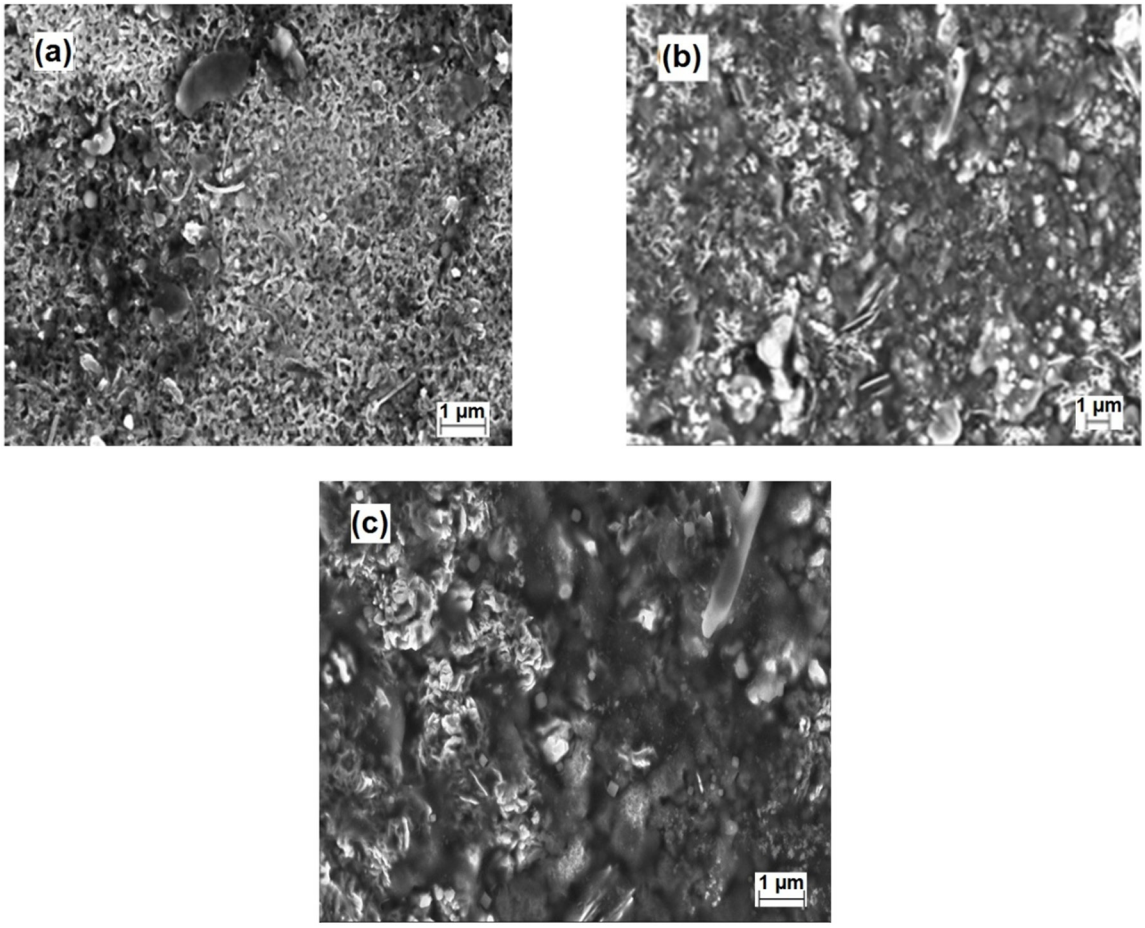

Figure 8. HRSEM micrograph of samples treated at 950 °C for (a) 30 min, (b) 60 min and (c) 90 min.

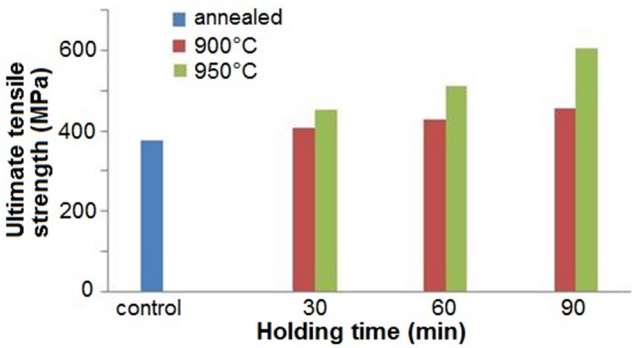

Figure 9. Variation of ultimate tensile strength (MPa) with holding time (mins) at 900 °C and 950 °C.

According to figure 9, it is obvious that the ultimate tensile strength increased with increase in holding time and annealed temperature from 30–90 min and 900–950 °C, respectively. This can be due to the dissociation of CNTs, solubility of carbon in the sample as well as the rate of diffusion of the dissociated carbon at nano-size onto the surface of the sample. It is a known fact that carbon is one of the principal elements responsible for the mechanical properties of steel. Although the ductility of steel decreases with increase in carbon content, conversely in this study, significant increase in the tensile strength and hardness was observed. These results revealed that direct linear relationship exist between the holding time and rate of diffusion of the dissociated carbon onto the sample surface at the interface between the sample and the coating. This diffused carbon may possibly occupy the interstitial spaces in the sample surface and sub-surface, thereby acting as a barrier to the movement of dislocation and thus increasing the amount of stress required for the sample to deform. Comparing the results of coated samples treated at different temperatures, it can be concluded that the rate of diffusion increases with increase in temperature as was observed from the weight of the samples recorded after treatment at different holding times (not shown). The results further show that at almost equal weight, there was decrease in the coating thickness as the holding time increased especially for samples treated at 950 °C. The observed trend may be attributed to high rate of evaporation of the CNT/GA/water slurry from the coated mild steel as well as the dissociation of carbon at higher temperature. All the treated samples experienced yielding during the tensile strength test. The average of the upper and lower yield strengths were presented in table 3. As observed with tensile strength, the yield strength also increased with increase in holding time irrespective of the annealed temperature. This trend was expected as annealing treatment caused the softening of metallic materials. However, the cooling rate of coated mild steel was slowed to prevent the formation of marten-site, bainite or even fine pearlite microstructures, which contribute to hardness or toughness of a material. It

Table 3. Variation of corrosion current, corrosion rate and coating efficiency with holding time.

Treatment condition		β_a	β_c	i_{corr}	Corrosion rate	Polarization	Coating
°C	min	(V dec^{-1})	(V dec^{-1})	(A cm^{-2})	(mm yr^{-1})	resistance (Ω)	efficiency (%)
Control		0.433	0.213	0.005	65.674	10.970	—
900	30	0.262	0.182	0.002	28.505	18.971	56.596
900	60	0.253	0.166	0.002	24.587	20.538	62.562
900	90	0.290	0.182	0.002	17.746	31.801	72.978
950	30	0.310	0.134	0.002	19.514	24.209	70.286
950	60	0.275	0.134	0.001	16.601	27.380	74.721
950	90	0.264	0.109	0.001	13.286	29.259	79.769

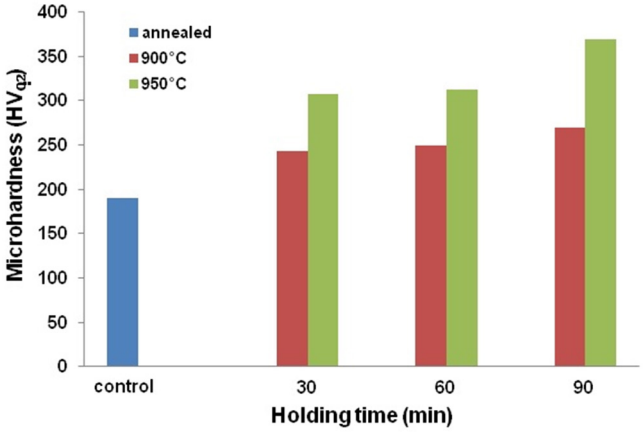

Figure 10. Variation of microhardness with holding time at 900 °C and 950 °C.

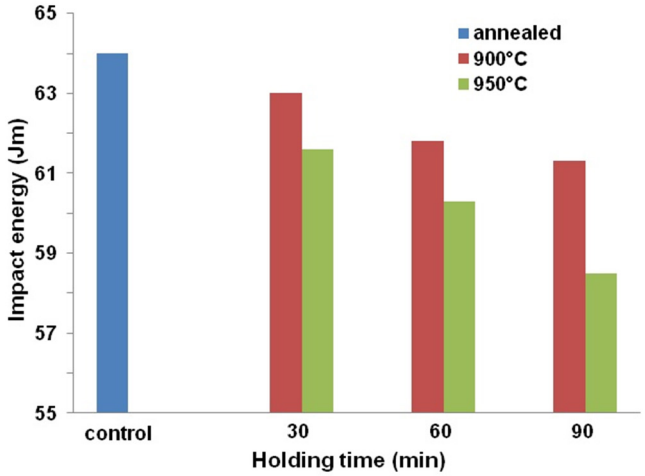

Figure 11. Variation of impact energy (Jm) with holding time (min) at different coating temperatures.

can also be seen from table 3 that both percentage elongation and reduction in area decreased with increase in holding time and temperature. Additionally, a mere visual inspection of the mild steel samples revealed that the coated and annealed mild steel at 900 °C and 950 °C for 90 min holding time pilled off at some points, which perhaps suggests the existence of weak electrostatic force of attraction between the mild steel and CNTs/GA/water system. Furthermore, the observed increase in the ultimate tensile strength and the yield strength with increase in holding time can be ascribed to the network properties of the CNTs and the GA on the surfaces of the mild steel. According to Peng *et al* [30] and Ferro *et al* [31] the tensile strength of MWCNTs is approximately 60 GPa, which enable it to withstand strain, torsion and bending without breaking.

The result of micro-hardness test is presented in figure 10 and it is seen that the micro hardness of the coated sample surfaces increased with increase in holding time at the temperatures under study.

Comparing the microhardness at different coating conditions, it is evident that the micro hardness of the surfaces also increases with increase in the treatment temperatures from 900 °C to 950 °C. The increase in micro hardness of the surfaces was due to the reaction between the detached carbon from the CNTs and the surface of the mild steel at the treatment temperature resulting to formation of Fe_3C and other carbides at the interface between the CNTs coating and the sample surface [32]. Thus, increase in holding time allowed sufficient amount of carbon to be dissociated from the tubes, permitting more carbon atoms to be diffused onto the steel surfaces, which increased the thickness of the carbide formed at the interfaces thereby resulting to more resistant to indentation at the skin. The impact strength of the treated coated and annealed samples was also investigated and the result obtained is presented in figure 11. From figure 11, it can be seen that the impact strength of the coated samples slightly decreased with increase in holding time. In the case of samples treated at 900 °C, the impact strength decreased by 2.70% from 63 Jm at the holding time of 30 min to 61.3 Jm for the holding time of 90 min. Similarly, for the sample annealed at 950°C, the measured impact strength for 30 and 90 min were 61.6 and 58.5 Jm, respectively, which corresponds to 5.03% reduction in impact strength.

Comparing the samples treated at 900 °C and 950 °C, it is apparent that the decrease in impact strength was more at 950 °C than 900 °C. During the test, it was noticed that some parts of the coating cracked and detached from the surface of the mild steel especially at 900 °C. Again, the toughness was found to decrease slightly, the possible reason can be linked to the treatment method (annealing), which allowed slower cooling rate resulting to formation of soft and ductile coarse grains. The percentage elongation of a material is the measure of the material extension under loading as compared to the initial length of the material.

Figure 12 shows that the percentage elongation decreased from 27 to 24.7% as the temperature increased from 900 °C to

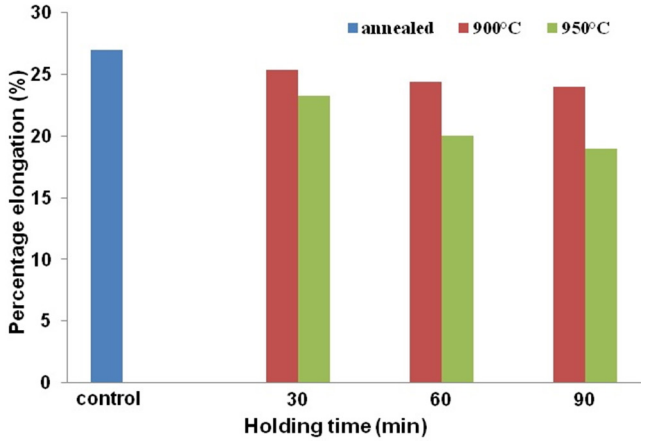

Figure 12. Variation of percentage elongation (%) with holding time (min) at 900 °C and 950 °C.

950 °C at 30 min holding time. The result also shows that the elongation decreased further from 25 to 20% and from 25 to 18.6%, as the holding time increases from 30 to 90 min at the treatment temperature of 900 °C and 950 °C, respectively. This indicates that the rate of diffusion of carbon depends on both temperature and holding time. As the diffusion rate increased more carbon gets to the sub-surface and hindered the movement of dislocation, which resulted to increase in the tensile strength and hardness, as a consequence, reduction in ductility. This also explains the decreased in the percentage reduction in area with increased holding times and temperatures.

3.4. Electrochemical corrosion behaviour of the coated mild steel in acidic medium

The electrochemical corrosion behaviour of the coated mild steel samples was studied when immersed in 0.5 M H_2SO_4 and the Tafel plots of these samples at different coating conditions in this medium are shown in figure 13. The polarisation parameter such as Tafel slope for the anodic and cathodic reactions, corrosion current, corrosion rate and the corrosion resistant were evaluated from the Tafel curves, summarized and tabulated in table 3.

The results of the corrosion behaviour of these samples are presented in form of curves usually referred to as Tafel polarization curves shown in figure 13. These curves exhibit linear behaviour in the E versus log$i$ plots called Tafel behaviour. The E_{corr} and i_{corr} were determined by extrapolation of the slope of the polarization curves back to the corrosion potential, the intersection point corresponds to corrosion current density i_{corr} or corrosion rate and the corresponding potential at that point is the E_{corr}. The slope of the potential-current density plot near E_{corr} is defined as polarization resistance (R_p) also expressed as shown in equation

$$R_p = \frac{\Delta E}{\Delta i}. \tag{3}$$

Mathematically, the corrosion current (i_{corr}) can be calculated from the Stean Geary relationship in equation

$$R_p = \frac{\beta_a \beta_c}{2.303(\beta_a + \beta_c) i_{corr}}, \tag{4}$$

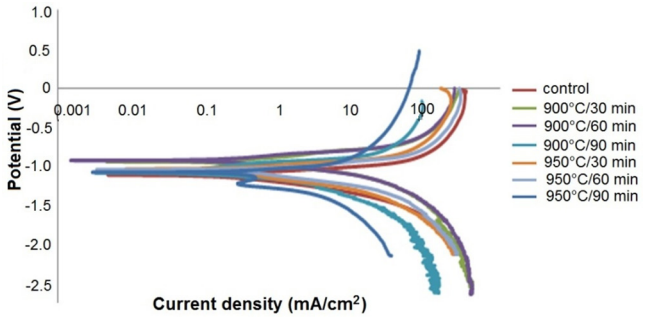

Figure 13. Polarisation curve for uncoated and coated samples at different coating conditions.

where β_a (V dec^{-1}) and β_c (V dec^{-1}) are the Tafel constants from the slopes of anodic and cathodic reaction curves, respectively, and i_{corr} (A cm^{-2}) is the corrosion current density. The corresponding corrosion rate (CR) can be obtained from equation

$$\mathrm{CR} = \frac{i_{corr} M}{\mathrm{DZF}}, \tag{5}$$

where M is the molecular weight of steel (=55.847 g mol^{-1}), D is the density of steel (=7.874 kg m^{-3}), Z is valence state of iron metal in oxidized form (=2) and F is Faraday's constant. The coating efficiency (CE) can be calculated from the expression in equation

$$\mathrm{CE}(\%) = \frac{i_o - i_a}{i_a} \times 100, \tag{6}$$

where i_a is corrosion current for the annealed (uncoated) mild steel sample, i_o is the corrosion current for the coated mild steel samples at different coating conditions [33].

From the polarization scans in figure 13, a slight shift in polarisation potential value for the coated samples were observed compared to the uncoated samples. This shift in corrosion potential value signifies barrier type of corrosion protection as it was in the positive direction of the potential. The shift in corrosion potentials was not observed in the order of either the coating thickness or the coating conditions. This is because the Tafel curve for sample coated at 900 °C for 60 min shows more shift towards the least negative potential, which suggests that the barrier is ineffective when the ion concentration is large [34]. The deviation in the shape of the curves indicates that both anodic and cathodic reactions were inhibited as evident in the anodic and cathodic slope constant values. Furthermore, table 3 shows that the respective corrosion currents and corrosion rates decrease from 0.002 46 to 0.001 75 (A cm^{-2}) and from 28.505 to 20.333 (mm yr^{-1}) with increase in holding times from 30 to 90 min at 900 °C heating temperature respectively, thus resulted to increase in the coating efficiency. Similar trend was observed for samples annealed at 950 °C for different holding times. There was a reduction in the corrosion current density and corrosion rate from 0.001 6828 to 0.001 145 699 (A cm^{-2}) and 19.514 38 to 13.285 95 (mm yr^{-1}), respectively, as the holding times increased from 30 to 90 min, respectively. Comparing the corrosion rates at different temperatures, it is possible to conclude that the lowest corrosion rate was observed on sample coated at 950 °C for 90 min. The corrosion results obtained in

this study can be attributed to the amount of carbon diffusion onto surface and sub-surface of the mild steel which increased as the holding time and treatment temperature increased [35]. It is however noteworthy to mention that CNTs are either metallic or n or p-type semiconductor. For instance, Orazem *et al* [36] and Harrington and Devine [37] buttressed that the n-type semiconductor in the form of oxide has the ability to impede the migration of anion (–OH) toward the metal surface. Based on this, the CNTs film effectively increased the negative charge on the samples surface, thereby impeding an anodic reaction of the form, $Fe \rightarrow Fe^{2+} + 2e^{-}$, thus decreased the rate of corrosion [38]. The observed slightly high corrosion rates were due to the presence of defects and pores as evidenced in the surface morphology (figure 8). These defects and pores allowed the electrolyte diffusion, thus promoting the failure of the protective barrier [39].

4. Conclusions

In this study, the mechanical properties and corrosion behaviour of mild steel coated with MWCNTs at different coating conditions were investigated. Based on the HRSEM/HRTEM analyses, multi-walled carbon nanotubes were successfully prepared from a bimetallic catalyst of Fe–Ni supported on gamma alumina support via conventional chemical vapour deposition reactor using acetylene carbon source. The ultrasonication process was employed in the dispersion of MWCNTs in GA and was responsible for the significant reduction in the diameters of the purified MWCNT bundles from the range of 500–3800 nm to the level of thin rope having diameter between 100 and 300 nm. The coating thickness decreases as the coating temperature and holding time increased. The tensile strength, yield strength, hardness value of the coated steel samples increased with increase in coating temperature and holding time while the impact energy showed slight decrease with increase in coating temperature and holding time. The coated mild steel samples at the temperature of 950 °C for 90 min holding time showed the best combination of hardness, yield strength and tensile strength values which however resulted to having slightly lower impact energy value as compared to samples treated at other different conditions. A reduction in the corrosion current and corrosion rate of the coated mild steel samples was observed with an increase in holding time and coating temperature whereas the polarization resistant and the coating corrosion efficiency increased with coating temperature and holding time. The lowest corrosion rate was observed on sample coated at 950 °C for 90 min.

Acknowledgments

Support received from Tertiary Education Trust Fund (TETFund) of Nigeria under a grant number TETFUND/FUTMINNA/2014/025 is highly appreciated. Centre for Genetic Engineering and Biotechnology (CGEB) FUTMinna is also appreciated for providing direct access to the centre facilities

References

[1] Kulka M, Mikolajczak D, Makulu N, Dziarski P and Miklaszewski A 2016 *Surf. Coat. Tech.* **291** 293
[2] Sivkov A, Shakenkov I, Park A, Geracimov D and Shanenkwa Y 2016 *Surf. Coat. Tech.* **291** 1
[3] William D C and David G R 2009 *Material Science and Engineering: an Introduction* 8th edn (New York: Wiley) pp 141–55
[4] Vytautas Č, Antanas A, Jonas V and Valdas K 2010 *Mater. Sci.* **16** 1392
[5] Oyetunji A and Adeosun S O 2012 *J. Basic Appl. Sci.* **8** 319
[6] Philip A S 2010 *Fundamental of Corrosion; Mechanism, Causes and Preventive Methods* (Boca Raton, FL: CRC Press) pp 14–25
[7] Singh B P, Jena B K, Bhattacharjee S and Besra L 2013 *Surf. Coat. Tech.* **232** 475
[8] Rani B E A and Basu B J 2011 *Int. J. Corros.* **20** 380217
[9] Montemor M F 2011 *Surf. Coat. Tech.* **258** 17
[10] Visser P, Liu Y, Terryn H and Mol J M C 2016 *J. Coat. Technol. Res.* **13** 557
[11] Iijima S 1991 *Nature* **354** 56
[12] Tripathi S M, Bholanath T S and Shantkriti S 2010 *Int. J. Control Autom.* **3** 53
[13] Moisala A, Nasibulin A G, Shandakov S D, Jiang H and Kauppinen E I 2005 On-line detection of single-walled carbon nanotube formation during aerosol synthesis methods *Carbon* **43** 2066
[14] Chen X H, Chen C S, Xiao H N, Cheng F Q, Zhang G and Yi G J 2005 *Surf. Coat. Tech.* **191** 351
[15] Poole C P and Owens F J 2003 *Introduction to Nanotechnology* (New York: Wiley) pp 196–200
[16] Goyal R, Chawla V, Sidhu B S and Singh K 2012 *IJRMET* **2** 55
[17] Qi T, Hashinocto T, Walton J R, Zhou X, Skeldin P and Thompson G E 2015 *Surf. Coat. Tech.* **270** 317
[18] Marder A R 2000 *Prog. Mater. Sci.* **45** 191
[19] Tiwari S K, Mishra T, Gunjan M K, Bhattacharyya A S, Singh T B and Singh R 2007 *Surf. Coat. Tech.* **201** 7582
[20] Osarolube E, Owate I O and Oforka N C 2008 *Sci. Res. Essays* **3** 224
[21] Kumar M and Ando Y 2008 *Nano Lett.* **8** 463
[22] Meyers M A and Chawla K K 1999 *Mechanical Behavior of Materials* (Cambridge: Cambridge University Press)
[23] Kumar M 2011 *Carbon nanotube synthesis and growth mechanism Carbon Nanotubes—Synthesis, Characterization, Applications* ed S Yellampalli (Croatia: InTech)
[24] Saifuddin N, Raziah A Z and Junizah A R 2013 *J. Chem.* 18
[25] Peng C M, Naveed A S, Gad M and Jang K 2010 *Composites* A **41** 1345
[26] Xin X, Xu G and Li H 2013 *Dispersion and Property Manipulation of Carbon Nanotubes by Self-Assemibles of Amphiphilic Molecules* (Croatia: InTech) ch 10
[27] Dresselhaus M S 2004 *Mater. Today Mag.* **5** 48
[28] Zhu J, Kim J, Peng H, Margrave J L, Khabashesku V N and Barrera E V 2003 *Nano Lett.* **3** 1107
[29] Islam M F, Rojas E, Bergey D M, Johnson A T and Yodh A G 2003 *Nano Lett.* **3** 269
[30] Peng B, Locascio M, Zapol P, Li S, Mielke M L, Schatz G C and Espinosa D H 2008 *Nat. Nanotechnol.* **3** 626
[31] Ferro G, Tulliani J M and Musso S 2011 Carbon nanotubes cement composites *Proc. Cassino (FR), Italia* pp 49–59
[32] Jianhua Y, Qunli Z, Mingxia G and Zhang W 2008 *J. Appl. Surf. Sci.* **254** 7092

[33] Peng W, Shanhao Z, Xinghina Z, Kaixuan G, Xingxia L, Jiading A and Wenbo H 2016 *Surf. Coat. Tech.* **230** 330
[34] Castro Y, Ferrari B, Moreno R and Duran A 2005 *Surf. Coat. Tech.* **19** 228
[35] Datsyuk V, Landois P, Fitremann J, Peigney A, Galibert A M, Soula B and Flahaut E 2009 *J. Mater. Chem.* **19** 2729
[36] Orazem M E, Pebere N and Tribollet B 2006 *J. Electrochem. Soc.* **133** B129–36
[37] Harrington S P and Devine T M 2009 *J. Electrochem. Soc.* **156** 154
[38] Sreeya S 2009 Carbon nanotube electronic structures as anti-corrosion coatings *PhD Thesis* New Jersey Institute of Technology and Rutgers, The State University of New Jersey, Newark
[39] Abu-Dalo M A, Othman A A and Al-Rawashdeh N A 2012 *Int. J. Electrochem. Sci.* **7** 9303